Limnology and Oceanography
October 2021, Volume 66, Issue 10, Pages 3682-3696
https://doi.org/10.1002/lno.11909
https://archimer.ifremer.fr/doc/00718/83017/

Inorganic and organic carbon and nitrogen uptake strategies of picoplankton groups in the northwestern Atlantic Ocean

Berthelot Hugo [1, 2, *], Duhamel Solange [3, 4], L'Helguen Stéphane [1], Maguer Jean-Francois [1], Cassar Nicolas [1, 5, *]

[1] Laboratoire des Sciences de l'Environnement Marin (LEMAR), UMR 6539 UBO/CNRS/IRD/IFREMER Institut Universitaire Européen de la Mer (IUEM) Brest ,France
[2] Sorbonne Université, CNRS Station Biologique de Roscoff, AD2M, UMR Roscoff,France
[3] Division of Biology and Paleo Environment Lamont-Doherty Earth Observatory Palisades New York, USA
[4] Department of Molecular and Cellular Biology The University of Arizona Tucson Arizona, USA
[5] Division of Earth and Ocean Sciences, Nicholas School of the Environment Duke University Durham North Carolina ,USA

* Corresponding authors : Hugo Berthelot, email address : hugo.berthelot@gmail.com ; Nicolas Cassar, email address : nicolas.casssar@duke.edu

Abstract :

Picoplankton populations dominate the planktonic community in the surface oligotrophic ocean. Yet, their strategies in the acquisition and the partitioning of organic and inorganic sources of nitrogen (N) and carbon (C) are poorly described. Here, we measured at the single-cell level the uptake of dissolved inorganic C (C-fixation), C-leucine, N-leucine, nitrate (NO_3^-), ammonium (NH_4^+), and N-urea in pigmented and nonpigmented picoplankton groups at six low-N stations in the northwestern Atlantic Ocean. Our study highlights important differences in trophic strategies between Prochlorococcus, Synechococcus, photosynthetic pico-eukaryotes, and nonpigmented prokaryotes. Nonpigmented prokaryotes were characterized by high leucine uptake rates, nonsignificant C-fixation and relatively low NH_4^+, N-urea, and NO_3^- uptake rates. Nonpigmented prokaryotes contributed to 7% ± 3%, 2% ± 2%, and 9% ± 5% of the NH_4^+, NO_3^-, and N-urea community uptake, respectively. In contrast, pigmented groups displayed relatively high C-fixation rates, NH_4^+ and N-urea uptake rates, but lower leucine uptake rates than nonpigmented prokaryotes. Synechococcus and photosynthetic pico-eukaryotes NO_3^- uptake rates were higher than Prochlorococcus ones. Pico-sized pigmented groups accounted for a significant fraction of the community C-fixation (63% ± 27%), NH_4^+ uptake (47% ± 27%), NO_3^- uptake (62% ± 49%), and N-urea uptake (81% ± 35%). Interestingly, Prochlorococcus and photosynthetic pico-eukaryotes showed a greater reliance on C- and N-leucine than Synechococcus on average, suggesting a greater reliance on organic C and N sources. Taken together, our single-cell results decipher the wide diversity of C and N trophic strategies between and within marine picoplankton groups, but a clear partitioning between pigmented and nonpigmented groups still remains.

Introduction

Primary production is limited by nitrogen (N) availability in large portions of the world ocean (Moore et al. 2013). The scarcity of N resources selects for smaller phytoplankton with larger surface-area-to-

volume ratio. This strategy is believed to explain the biomass dominance of picoplankton (< 3 µm) in oligotrophic regions (Marañón 2015). Picoplankton encompass a great diversity of populations and ecological functions (Massana 2011) but when analyzed using flow cytometry the populations generally cluster in well-defined groups including the pigmented photosynthetic groups of prokaryotes *Prochlorococcus* and *Synechococcus* and pico-eukaryotes, as well as the non-pigmented prokaryotes. These groups are present in the surface ocean in variable abundances and proportions depending on environmental factors such as temperature, light and nutrient supply (Otero-Ferrer et al. 2018). *Prochlorococcus* is present at latitudes lower than 45°N/S and numerically dominates the phytoplankton communities in oligotrophic and warm waters such as the subtropical gyres. *Synechococcus* is more widespread and is observed in nearly all the surface waters of the world ocean with the exception of the Arctic and Southern Oceans. As opposed to *Prochlorococcus*, *Synechococcus* is most abundant in temperate and relatively mesotrophic waters (Flombaum et al. 2020). Photosynthetic pico-eukaryotes are ubiquitous in the oceans and their biomass generally dominate over *Prochlorococcus* and *Synechococcus* in nutrient rich water and at high latitudes (Flombaum et al. 2020). They harbor a great diversity of organisms (including Prasinophyceae, Mamiellophyceae, Haptophyceae, Chrysophyceae, Pelagophyceae) making this group heterogeneous (Hernández-Ruiz et al. 2018; Mucko et al. 2018). Non-pigmented prokaryotes in surface layers of the oceans are also diverse, mostly composed of bacteria (>90%) (Ibarbalz et al. 2019), which are ubiquitous in the ocean at relatively high abundances (10^5-10^6 cells ml^{-1}) (Du et al. 2006).

Pigmented groups have traditionally been hypothesized to exclusively use dissolved inorganic carbon (C) as their source of C, and sunlight as a source of energy to fix C via photosynthesis (photoautotrophy). Conversely, non-pigmented prokaryotes are conventionally described as pure heterotrophs, i.e. relying on organic C for their growth, playing a key role in the remineralization of organic matter (Azam 1998). However, this idealized conceptual model is questioned by a growing body of evidence showing that mixed trophic regimes are a common feature in the ocean. Some pigmented organisms use organic C as sources of C and energy in addition to dissolved inorganic C, a trophic strategy called mixotrophy. The organic C acquisition can be mediated by a direct uptake of dissolved compounds (osmo-mixotrophy)

or by predation on prey (phago-mixotrophy) (Sanders and Gast 2012; Hartmann et al. 2012; Muñoz-Marín et al. 2020). Recent studies have demonstrated the high affinities of several pigmented species for dissolved organic substances, leading to a potential for resource competition with pure heterotrophs (Kamjunke et al. 2008). As an example, the complete gene pathways for glucose acquisition, and small but significant uptake rates have recently been found in *Prochlorococcus* and *Synechococcus* (Muñoz-Marín et al. 2020). Similarly, the use of dissolved inorganic C by non-pigmented organisms through chemoautotrophic processes has been reported in communities present in oceanic surface waters (Middelburg 2011).

This partitioning between organic and inorganic resources is also relevant to N acquisition. While the former traditional view is that pigmented organisms mostly rely on inorganic N, mainly ammonium (NH_4^+) and nitrate (NO_3^-), and non-pigmented prokaryotes on organic N substrates, including amino-acids, a number of studies have shown that the N strategies between the two trophic regimes are not completely distinct. In the N-rich sub-Arctic Pacific, non-pigmented prokaryotes have been shown to contribute to ~30% of the NO_3^- and NH_4^+ community uptake rates (Kirchman and Wheeler 1998). Comparable contributions (~40%) were found in a eutrophic coastal Mediterranean lagoon (Trottet et al. 2011) and in Sub-Arctic Atlantic (Fouilland et al. 2007) while much smaller (4-14%) were observed in the post-bloom temperate waters of the North Atlantic (Kirchman et al. 1994). In parallel, an increasing number of studies show that photosynthetic organisms use Dissolved Organic N (DON) compounds for their growth (Bronk et al. 2007). For example, urea is thought to fuel the recurrent harmful algal blooms of *Aureococcus anophagefferens* (Berg et al. 1997). The ability of *Prochlorococcus* to use dissolved free amino acid has been hypothesized to explain its dominance in oligotrophic waters where inorganic N is depleted (Zubkov et al. 2003).

Despite the growing body of evidence for the prevalence of mixed nutritional strategies and the clear implications for N and C resource competition, few studies have simultaneously investigated the uptake of organic and inorganic N and C by pigmented and non-pigmented planktonic communities (Bradley et al. 2010). The lack of observations can in part be explained by the methodological challenge of measuring these processes *in situ* at the plankton group scale. The most common approach combines

stable or radioactive isotope labelling and post incubation size fractionation where large and small size fractions are attributed to photosynthetic groups and non-pigmented prokaryotes, respectively, with a typical cut-off at 0.7-1 µm (Kellogg and Deming 2009; Schapira et al. 2012). However, retention of non-pigmented prokaryotes in the largest size fractions has been shown to be significant, in particular embedded in aggregates and/or attached to the cell surface of large organisms (Seymour et al. 2017). Similarly, the smallest pigmented groups, such as *Prochlorococcus* or *Ostreococcus*, are within the size spectrum of non-pigmented prokaryotes leading to an overall poor specificity of size fractionation, particularly in open ocean waters where small cells dominate photosynthetic communities (Casey et al. 2019). Inhibitors specific to plankton groups have also been used to assess the contribution of prokaryotes to the uptake of inorganic nutrients (Fouilland et al. 2007). However, the efficiency and the specificity of the inhibitors in natural planktonic communities is questionable (Oremland and Capone 1988). Flow cytometric cell sorting has been used in combination with radioactive isotope labelling allowing the determination of uptake rates of inorganic or organic substances labelled with ^{14}C, ^{33}P, ^{35}S or ^{3}H at the group-level (e.g. Jardillier et al. 2010; Duhamel et al. 2019). Approaches using radioactive isotopes present the advantage of higher sensitivity than stable isotopes. They have been used to evidence group specific patterns such as the in-situ *Prochlorococcus* uptake of amino acids (Muñoz-Marín et al. 2020), the ingestion of non-pigmented prokaryotes cells by photosynthetic pico-eukaryotes (Hartmann et al. 2012; Duhamel et al. 2019) or the faster growth of *Prochlorococcus* and *Synechococcus* compared to photosynthetic pico-eukaryotes (Zubkov 2014). Unfortunately, there is no suitable radioactive tracer for N.

In this study, we circumvent these methodological issues by coupling dual stable isotope labelling assays (^{13}C, ^{15}N) with flow cytometry cell sorting and nanoSIMS to measure at the single cell level the use of inorganic (dissolved inorganic C, NH_4^+ and NO_3^-) and organic (urea, leucine) sources of N and C by *Prochlorococcus*, *Synechococcus*, photosynthetic pico-eukaryotes and non-pigmented prokaryotes. We applied our approach in various biomes of the northwestern Atlantic, from the subtropical gyre to the Gulf Stream and Labrador Current. A common characteristic of these regions is a general state of nitrogen or phosphorus limitation (Wu et al. 2000; Lipschultz 2001; Moore et al. 2008). While

wintertime mixing can bring NO_3^- and phosphate (PO_4^{3-}) rich waters to the surface (even in the oligotrophic waters near Bermuda), summer stratification leads to a reduction in nutrient availability in oceanic and coastal waters to levels limiting primary production as demonstrated by nutrient addition bioassays, in particular for N (Sedwick et al. 2018). This study provides a direct *in situ* comparison of N and C uptake by pigmented and non-pigmented picoplankton at the single cell level, highlighting the contrasting nutritional strategies sustaining the growth of specific picoplankton groups in the ocean.

Materials

Sampling and biogeochemical analyses

The study was conducted in the northwestern Atlantic between Bermuda and the United States New England coast aboard of the R/V *Atlantic Explorer* in August 2017. Six stations with contrasting biogeochemistry were sampled: two stations in the North Atlantic Gyre (stations A and B) among which one is the Bermuda Atlantic Time-series Study (BATS) station (hereafter Station A), two stations in the Gulf Stream (stations C and D) and two stations on the continental shelf of the coast of New England (stations E and F) (Fig. 1). Surface seawater samples (5 m) were collected using Niskin bottles mounted on a rosette equipped with CTD sensors. At each station, samples for dissolved N nutrients were collected in triplicate and filtered through combusted GF/F filters (4h, 450°C) before being stored at -20°C until further analysis. Care was taken to copiously rinse the filters with ultrapure water and seawater before sampling in order to avoid contaminations. Samples for NO_3^-, urea and PO_4^{3-} were collected in acid cleaned (soaked in hydrochloric acid 10%, followed by ultrapure water three times) polypropylene tubes (50 mL or 15 mL) and measured colorimetrically according to Raimbault et al. (1990), Mulvenna and Savidge (1992) and Strickland and Parsons (1972), respectively. The limits of detection were 10, 60 and 14 nmol N L^{-1} for NO_3^-, urea and PO_4^{3-}, respectively. Samples for NH_4^+ were collected in 50 mL polypropylene tubes which were conditioned beforehand to reduce risks of contamination: the tubes were first left overnight in hydrochloric acid 10%, rinsed three times with freshly produced ultrapure water and filled in a mixture of ultra-pure water and reagents for NH_4^+ determination until sampling. Samples were then measured fluorimetrically as described in Holmes et

155 al. (1999) with standards made from NH_4^+-free deep seawater stored in the same conditions as samples.
156 The limit of detection was 3 nmol N L^{-1}.

157 ***Experimental design***

158 At each station, uptake of dissolved inorganic C (hereafter referred to as C-fixation), NH_4^+, NO_3^-, urea
159 and leucine were measured using stable isotope tracer incubations both at the plankton-community and
160 at the single-cell levels. For this purpose, seawater was collected at each station from the Niskin bottles
161 in four sets of five acid-cleaned 1.2 L polycarbonate bottles. Isotope-labelled tracers were added in all
162 the bottles directly after collection as follow: ^{13}C was added under the form of dissolved inorganic C
163 ($NaH^{13}CO_3$, 99%, Eurisotop) together with either $^{15}NO_3^-$ (KNO_3, 98%, Eurisotop), $^{15}NH_4^+$ (NH_4Cl, 98%,
164 Eurisotop) or ^{15}N-urea (98%, Eurisotop) or under the form of dual-labeled ^{13}C-^{15}N leucine (99% ^{13}C and
165 98% ^{15}N). C-fixation rates were calculated from the average of incubations performed in the presence
166 of $^{15}NO_3^-$, $^{15}NH_4^+$ and ^{15}N-urea. Isotopes were added to a final concentration of 30 nmol N L^{-1} for NH_4^+,
167 NO_3^- and urea at the gyres and at the Gulf Stream stations and 50 nmol N L^{-1} at the continental shelf
168 stations. Due to expected relatively low uptake rates, leucine was added at the saturating (or close to
169 saturating) concentrations of 10 nmol L^{-1} at all stations to ensure significant isotopic enrichments (Hill
170 et al. 2013). In order to determine the initial ^{13}C and ^{15}N isotopic abundance in the particulate matter,
171 one bottle from each set was filtered onto combusted GF/F (4 h, 450 °C) directly after the addition of
172 the isotopes. Filters were rinsed with 0.2 µm pore-size filtered seawater and stored at -20 °C. The
173 remaining bottles from the set were placed in an on-deck incubator reproducing the light intensity at the
174 surface and kept at sea surface temperature by a continuous circulation of surface seawater. The
175 incubations lasted 3–8 h (5.5 h on average), except for the leucine treatments for which incubations
176 lasted 22–24 h in order to ensure significant isotopic enrichments. Incubations were stopped by filtering
177 three of the four remaining bottles from each set onto combusted GF/F as described above. The last
178 bottle from each set was used to concentrate the cells for flow cytometry cell sorting. For this purpose,
179 the bottle content was filtered onto 0.2 µm polycarbonate filters. The filtration was stopped just before
180 the filter went dry and ~10 mL of 0.2 µm filtered sea water with PFA (1.6% final concentration) was
181 added on the filter and left for 1 h in the dark. The solution was then filtered, the filters were placed in

5 mL cryotubes filled with 0.2 µm filtered seawater. The cryotubes were vortexed in order to resuspend the cells in the solution, then flash frozen in liquid N_2 and stored at -80°C.

Flow cytometry cell sorting and isotopic analyses

Flow cytometry cell sorting and nanoSIMS analyses were conducted as previously described in Berthelot et al. (2019) with a few modifications. Concentrated cells in cryotubes were sorted back onshore using a BD Influx cell sorter equipped with a 70 µm nozzle, with sheath fluid and sample fluid pressure of 30 PSI (207 kPa) and 31 PSI (214 kPa), respectively. The instrument was set at the highest sorting purity (1.0 drop single mode), the drop delay was calibrated using Accudrop Beads (BD Biosciences, USA) and the sorting efficiency was verified manually by sorting a specified number of 1 µm yellow–green microspheres (Polysciences #17154-10) onto a glass slide and counting the beads under an epifluorescence microscope. We systematically recovered 100% of the targeted beads before sorting samples. Using this setup, the sorting purity on our instrument typically exceeds 96% (Duhamel et al. 2019). *Prochlorococcus*, *Synechococcus* and photosynthetic pico-eukaryotes were discriminated in unstained samples while non-pigmented prokaryotes were discriminated in a sample aliquot stained with SYBR Green I DNA dye (0.01% final). non-pigmented prokaryotes clustered in two groups: low nucleic acid and high nucleic acid. Using a forward scatter detector with small particle option and focusing a 488 plus a 457 nm (200 and 300 mW solid state respectively) laser into the same pinhole allowed the resolution of dim surface *Prochlorococcus* population from background noise in unstained samples. However, in stained samples, *Prochlorococcus* overlapped with high nucleic acid group and therefore, only cells belonging to low nucleic acid group were sorted and further analyzed for isotopic ^{13}C and ^{15}N contents and are referred collectively as non-pigmented prokaryotes. Filters containing the sorted cells were analyzed on a CAMECA nanoSIMS 50 using a focused 1.2 pA Cs^+ ion beam scanning fields of 10 x 10 µm (for non-pigmented prokaryotes and *Prochlorococcus*), 20 x 20 µm (for *Synechococcus*) and 30 x 30 µm (for photosynthetic pico-eukaryotes) and recording alternatively the $^{12}C^{14}N^-$ and $^{12}C^{15}N^-$ or $^{12}C^{14}N^-$ and $^{13}C^{14}N^-$ secondary ions using the "peak jumping mode" over at least 20 planes. Mass resolution was >7,000 to resolve the $^{12}C^{15}N^-$ and $^{13}C^{14}N^-$ ions (See Berthelot et al. 2019 for further details). Cells were then identified based on the $^{12}C^{14}N^-$ total ion count images and outlined

using the particle detection mode of the LIMAGE software. Each particle detected was individually checked and redrawn if needed or discarded when it was not possible to attribute it to a cell with certainty. Particulate C and N concentrations and isotopic ratios at the community scale were determined on an isotope ratio mass spectrometer coupled to an elemental analyzer (EA-IRMS) from the triplicate GF/F filters. At the average C and N content measured on the samples (~6 µmol C and ~0.9 µmol N), the precision (standard deviation of repeated measurements) of the elemental analyses were 0.08 µmol C and 0.007 µmol N and the precision of the isotopic percent abundances were 0.0004 atom% and 0.0003 atom% for C and N, respectively.

Rate calculations and statistical analyses

For each cell analyzed, the isotopic percent abundances of ^{13}C ($A^{13}C = \frac{^{13}C^{14}N^-}{^{13}C^{14}N^- + {}^{12}C^{14}N^-} * 100$) and ^{15}N ($A^{15}N = \frac{^{12}C^{15}N^-}{^{12}C^{14}N^- + {}^{12}C^{15}N^-} * 100$) were used to calculate the element (C- or N-) specific uptake rate (h^{-1}):

$$element\ specific\ uptake = \frac{A_{cell} - \bar{A}_{t0}}{A_{source} - \bar{A}_{t0}} * \frac{1}{t}$$

where A_{cell}, $\overline{A_{t0}}$, and A_{source} are the isotopic percent abundances of the cell after incubation (A_{13C} or A_{15N}), of the cells (mean) prior to incubation, and of the source pool, respectively and *t* is the incubation time. Note that in the case of dissolved inorganic C, the specific uptake rates are termed C-specific C-fixation rate. In addition to C- and N-specific uptake rates, C-fixation based division rates were calculated as follows:

$$C\ fixation\ based\ division = log2\left(\frac{A_{source} - \bar{A}_{t0}}{A_{source} - A_{cell}}\right) * \frac{1}{t}$$

C-fixation based division rates reflect cellular division rates if inorganic C-fixation is the unique source of elemental C to the organism, as would be the case in case of exclusive photoautotrophy. For comparison with the literature, C-fixation division rates are presented in d^{-1}. As the incubations were not performed from dawn to dusk, hourly rates were converted to daily rates using the model developed by

Moutin et al. (1999) which account for the variation of daylight intensity at the sampling site and on the sampling day.

Cell-specific uptake rates (amol C cell^{-1} h^{-1} and amol N cell^{-1} h^{-1}) were calculated as follows:

$$cell\ specific\ uptake = \frac{A_{cell} - \bar{A}_{t0}}{A_{source} - \bar{A}_{t0}} * \frac{1}{t} * Q_{cell}$$

With Q_{cell} the estimated C and N cell contents. For pigmented organisms, C and N cell contents used were the median values reported by Baer et al. (2017) in northwestern Atlantic (5, 23 and 257 fmol C cell^{-1} and 0.6, 2.4 and 15 fmol N cell^{-1} for *Prochlorococcus*, *Synechococcus* and photosynthetic pico-eukaryotes, respectively). For non-pigmented prokaryotes, a C cell content of 1.7 fmol C cell^{-1} and a C:N ratio of 6.6 were used (Fukuda et al. 1998). The cell-specific uptake rates of dissolved inorganic C are termed cell-specific C-fixation rates. Group uptake rates were obtained by multiplying per-cell rates by cell abundances in the respective group.

Single cell uptake was considered to be above the detection limit when the percent abundance enrichment ($A_{cell} - \bar{A}_{t0}$) was higher than two times the standard deviation associated with the Poisson distribution (λ) parameterized as $\lambda = A_{cell} * N_{CN^-,cell}$, where $N_{CN^-,cell}$ is the CN^- ions counts of the cell. Similarly, groups were considered as active when the mean cellular percent isotopic abundances enrichment of the groups ($\bar{A}_{group} - \bar{A}_{t0}$) were two times higher than the standard deviation of the cellular percent abundances. Differences in C or N specific uptake between stations or groups were tested using unpaired Kruskal-Wallis test and considered significant if $p < 0.05$.

The community C and N uptake rates (nmol C L^{-1} h^{-1} or nmol N L^{-1} h^{-1}) were measured from GF/F filters as follows:

$$Commmunity\ uptake = \frac{A_{PM} - \bar{A}_{t0}}{A_{source} - \bar{A}_{t0}} * \frac{1}{t} * PM$$

With PM the particulate C or N concentration and A_{PM} the isotopic percent abundance of ^{13}C or ^{15}N in the particulate matter.

Due to the low concentrations of NH_4^+, NO_3^- and urea, isotopes tracers additions exceeded the threshold of 10% of the ambient concentrations for trace level additions. As a result, percent isotopic abundances in the source pool (A_{source}) ranged between 41-95%. Two uptake kinetics experiments with increasing nutrient additions at the gyre stations were performed to assess the extent of overestimation of the uptake due to the ^{15}N added. Rates were then corrected for this overestimation according to Harrison et al. (1996) to approximate *in situ* rates as much as possible. This correction resulted in a reduction of NH_4^+, NO_3^- and urea uptake rates by a factor 1.5, 2.4 and 1.1 on average, respectively. At stations were NO_3^- was below the detection limit, we assumed a NO_3 concentration of 5 nmol L^{-1} for the calculations. Leucine concentrations were not measured but assumed to be lower than 1 nmol L^{-1} (Zubkov et al. 2008) and uptake rates were calculated assuming percent isotopic abundances of ^{13}C and ^{15}N of 95% in the source pool. Leucine rates were not corrected from overestimation due to leucine addition at saturating (or close to saturating) concentrations and should thus be interpreted as "potential" rates. We did not correct for isotope dilution associated with regeneration of NH_4^+ during the incubations, which would tend to bias our estimates low. In order to limit this bias, the duration of the NH_4^+incubations were kept short (≤3.5 h). Minimum quantifiable rates were calculated at each station and for each tracer from the propagation of errors of the different parameters involved in the community uptake rate calculations according to Gradoville et al. (2017) (Table S1). All community uptake rates were higher than the minimum quantifiable rates. Maximal N fluxes constrained by diffusion-limited N supply to single cells were calculated from the analytical solutions of diffusion to a sphere:

$$\rho_{max} = 4\pi D r_0 (C_\infty - C_0)$$

where ρ_{max} is the maximal NH_4^+, NO_3^- or urea uptake rate (nmol s^{-1}) of a cell with the equivalent spherical radius r_0 (cm), D is the diffusion coefficient (cm^2 s^{-1}) of the considered compound in water, C_0 is the NH_4^+ concentration at the cell surface (assumed to be zero) and C_∞ is the measured concentration in the ambient water. We assume diffusion coefficients of 1.98 x 10^{-5}, 1.90 x 10^{-5} and 1.38 x 10^{-5} cm^2 s^{-1} at 25°C for NH_4^+, NO_3^- and urea, respectively (Longsworth 1963; Li and Gregory 1974).

Results

Biogeochemistry of the studied area

The biogeochemical characteristics of the sampled stations are presented in Table 1. At the time of sampling, surface NO_3^-, NH_4^+ and urea concentrations were low: NO_3^- was below the detection limit (10 nmol L^{-1}) and NH_4^+ and urea concentrations ranged between 11–28 nmol N L^{-1} and 91–173 nmol N L^{-1}, respectively, without clear patterns between regions. In contrast, PO_4^{3-} concentrations showed a strong pattern with higher concentrations at the continental shelf stations (110–152 nmol L^{-1}) than at the Gulf Stream (40–45 nmol L^{-1}) and the gyre (15-18 nmol L^{-1}) stations. In the surface waters of the gyre, Particulate C concentrations were ~2 µmol C L^{-1}. Particulate C concentrations were higher at the Gulf Stream stations (3–4 µmol C L^{-1}) and at the continental shelf stations (8–12 µmol C L^{-1}).

The cyanobacteria *Prochlorococcus* and *Synechococcus* dominated the surface pigmented pico-plankton community in the gyre with abundances in the same order of magnitude (~10^4 cell mL^{-1}), while photosynthetic pico-eukaryotes abundances were consistently lower than 5.10^2 cell mL^{-1} (Table 1). In the Gulf Stream, abundances were three times higher for photosynthetic pico-eukaryotes, three-to-seven times higher for *Synechococcus* and four-to-ten times higher for *Prochlorococcus* (which reached particularly high abundances at station C, >2.10^5 cell mL^{-1}) than in the gyre. At the continental shelf stations, *Prochlorococcus* was not detected, while *Synechococcus* abundances were in the range of those measured in the Gulf Stream and photosynthetic pico-eukaryotes were more abundant than in the two other regions studied. Non-pigmented prokaryotes abundances ranged between 2.10^5 to 6.10^5 cells mL^{-1} with the lowest abundances observed in the gyre. Among non-pigmented prokaryotes, two-subgroups were observed, characterized by their level of green fluorescence, which reflects their nucleic acid content: low nucleic acid and high nucleic acid content. Low nucleic acid sub-group numerically dominated the non-pigmented prokaryotes group at the gyre stations (59–63%) in contrast to the Gulf Stream and continental shelf stations (22–44%) (Table S2).

Community C-fixation in surface increased from the gyre (<20 nmol C L^{-1} h^{-1}) to the Gulf Stream (~60 nmol C L^{-1} h^{-1}) and to the continental shelf (>120 nmol C L^{-1} h^{-1}) (Table 1). Similarly, community NO_3^-

306 uptake rates were 0.4 nmol N L^{-1} h^{-1} in the GYR, 0.9–1.4 nmol N L^{-1} h^{-1} in the Gulf Stream and reached
307 as much as 3.8 nmol N L^{-1} h^{-1} at the continental shelf stations. Community NH_4^+ and N-urea uptake rates
308 were within the same range at each region (<1.8, 3.0–7.0 and 6.1–23.6 nmol N L^{-1} h^{-1}, at the gyre, Gulf
309 Stream and continental shelf stations, respectively). Community C- and N-leucine potential uptakes
310 rates were low in comparison to the other N compounds investigated (0.2–0.8 nmol C L^{-1} h^{-1} and 0.1–
311 0.3 nmol N L^{-1} h^{-1}, respectively) but followed the same regional trends with higher rates on the
312 continental shelf than in the Gulf Stream and gyre.

313 ***Single cell metabolic rates of the cytometrically sorted groups***

314 Single cell analyses of cytometrically sorted groups allowed the determination of the cellular fixation or
315 uptake rates of the ^{13}C or ^{15}N labelled substrates tested (Fig. 2, 3 and Table S3). The results are presented
316 in C- and N-specific uptake rates (h^{-1}) to allow for the comparison of metabolic activities between cells
317 with different biomass content. Cell-specific uptake rates (amol C $cell^{-1}$ h^{-1} and amol N $cell^{-1}$ h^{-1}) and C-
318 fixation based division rates (d^{-1}) are also presented in Table S3, S4 and Fig. S1 for comparison with
319 literature data. Intragroup C-specific C-fixation rates varied greatly, from undetectable to more than 0.1
320 h^{-1} (Fig. 2). However, when averaged, clear patterns appeared between the different groups sorted and
321 between regions. C-specific C-fixation was detected for a subset of the non-pigmented prokaryotes cells
322 (15% on average) but at the group scale significant activities were not detected at any stations (see
323 criteria in the experimental procedure section). In contrast, significant C-specific C-fixation was always
324 detected for pigmented groups (averaging 0.016±0.010, 0.022±0.015 and 0.016±0.012 h^{-1} for
325 *Prochlorococcus*, *Synechococcus* and photosynthetic pico-eukaryotes, respectively). C-specific C-
326 fixation rate was on average twice higher in the Gulf Stream than in the gyre for *Prochlorococcus*.
327 Similarly, *Synechococcus* displayed higher activity in the Gulf Stream and the continental shelf as
328 compared to the gyre. In contrast, no clear trends were observed between regions for photosynthetic
329 pico-eukaryotes.

330 When detected, C-specific leucine potential uptake rates were higher on average in non-pigmented
331 prokaryotes (0.0004±0.0002 h^{-1} on average) than in pigmented organisms (0.0001±0.0001 h^{-1} on

average). Among the pigmented groups, *Prochlorococcus* showed the highest C-specific leucine potential uptake rates and the highest proportion of active cells (0.0002±0.0055 h^{-1}, 53% of active cells), as compared to photosynthetic pico-eukaryotes (0.0001±0.0001 h^{-1}, 26% of active cells) and *Synechococcus* (<0.0001 h^{-1}, 14% of active cells), respectively, and no clear patterns were observed between regions (Fig. 2).

N-specific uptake rates were also highly variable between cells (Fig. 3). In the gyre and Gulf Stream regions where all three groups were detected, N-specific NH_4^+ uptake rate was on average slightly higher for *Synechococcus* (0.014±0.008 h^{-1}) than for *Prochlorococcus* (0.013±0.006 h^{-1}) and photosynthetic pico-eukaryotes (0.010±0.010 h^{-1}) and higher for pigmented groups (0.012±0.004 h^{-1}) than for non-pigmented prokaryotes (0.003±0.006 h^{-1}) (each group was significantly different from each other, $p<0.05$). N-specific urea uptake was the highest on average for *Synechococcus* (0.030±0.018 h^{-1}) followed by *Prochlorococcus* (0.023±0.016 h^{-1}), photosynthetic pico-eukaryotes (0.003±0.004 h^{-1}) and non-pigmented prokaryotes (0.003±0.002 h^{-1}), respectively (each group were significantly different from each other, $p<0.05$). N-specific NO_3^- uptake rates were on average higher for *Synechococcus* (0.006±0.005 h^{-1}) compared to photosynthetic pico-eukaryotes (0.001±0.002 h^{-1}), *Prochlorococcus* (0.001±0.003 h^{-1}) and non-pigmented prokaryotes (<0.001 h^{-1}), respectively (each group were significantly different from each other, $p<0.05$). Noticeably, at station C *Prochlorococcus* N-specific NO_3^- uptake peaked at 0.004±0.005 h^{-1}, a rate much higher than the one observed in photosynthetic pico-eukaryotes (0.002±0.003 h^{-1}). N-specific leucine potential uptake was an order of magnitude lower compared to the three other N substrates studied and was highest for non-pigmented prokaryotes (0.0013±0.0005 h^{-1}) as compared to the phytoplankton groups studied (0.0004±0.0004 h^{-1}, 0.0001±0.0001 h^{-1}, 0.0002±0.0003 h^{-1} for *Prochlorococcus*, *Synechococcus* and photosynthetic pico-eukaryotes, respectively).

At the intra group scale, the C-specific C-fixation uptake rates were relatively stable as a function of cell size. However, the higher C-specific C-fixation rate of *Synechococcus* lead to a peak of rates centered around 1 µm in equivalent spherical diameter when all the groups are considered together (Fig. 4). Cell size rates dependent patterns appeared more clearly at the intragroup levels for the other parameters

measured. Intriguingly, the N-specific uptake rates seemed to be more influenced by cell size rather than group identity. For NH_4^+, NO_3^- and N-urea patterns were similar with rates peaking for cells of size ca 1.5, 1.2 and 1.0 µm equivalent spherical diameter, respectively. For C- and N-specific leucine potential uptake rates, no peaks were observed but a decrease with increasing cell size.

Using C and N cell contents estimated from the literature and measured abundances, we computed groups' absolute rates and compared them to the community rates measured on the GF/F filters (Fig. 5). Pico-plankton (sum of non-pigmented prokaryotes, *Prochlorococcus*, *Synechococcus* and photosynthetic pico-eukaryotes) represented a significant fraction of the community C biomass (52±17% on average) and of the community C-fixation (63±27% on average) with large variability between stations (ranging from 35% to more than 100% of the community C-fixation). The contribution of groups to the community N species uptake was also noticeably variable between stations. For example, *Prochlorococcus* and photosynthetic pico-eukaryotes explained less than 10% of the community NO_3^- uptake, except at stations C and E, where these groups contributed to more than 55% of the community NO_3^- uptake. Similar patterns were also observed for NH_4^+ and N-urea uptake at these stations, which were explained by a conjunction of high abundances and high N-specific uptake. On average, the sum of pico-sized pigmented groups accounted for a relatively large fraction of NH_4^+ uptake (47±27%), NO_3^- uptake (62±49%) and N-urea uptake (80±35%). The contribution of non-pigmented prokaryotes to N uptake were much lower (averaging 7±3%, 2±2% and 9±5% for NH_4^+, NO_3^- and N-urea, respectively). In contrast, this group was the main contributor to the community N-leucine potential uptake (range 42-54%).

Discussion

Methodological considerations

The role of various groups of pico-plankton in ocean C and N cycling remains poorly resolved in part because of a lack of appropriate methodological tools. Since the first applications to environmental microbiology more than a decade ago, nanoSIMS coupled to isotope labelling assays has gained in popularity and has been used to measure the contribution of different microbial groups to the community

activity (Klawonn et al. 2016; Berthelot et al. 2019). Using this approach, we show in this study that picoplankton account for more than half of the community C-fixation in our study region (63% on average). This result is in line with previous measurements made in this area, and more generally in oligotrophic environments, using ^{14}C-sodium bicarbonate radioassays coupled with size fractionation or cell sorting (Jardillier et al. 2010; Duhamel et al. 2019). It is important to note that the cell-specific and group-specific uptake rates derived from nanoSIMS approaches rely on cell content data independently measured or reported in the literature which can vary by up to an order of magnitude between studies (Martiny et al. 2013; Baer et al. 2017). In our study, we used biomass cell contents measured from samples obtained in our sampling area, the northwestern Atlantic ocean (Baer et al. 2017). The derived cell-specific C-fixation rates (51–102, 317–806 and 2872–5388 amol C h^{-1} for *Prochlorococcus*, *Synechococcus* and photosynthetic pico-eukaryotes, respectively) are in good agreement with values recently reported in the literature (Jardillier et al. 2010; Zubkov 2014; Duhamel et al. 2019)(Fig. S1). These cell contents carry uncertainty (coefficient of variation of ±30% to >100%) which can affect the cell and group specific uptake rates to the same extent and may bias the estimated contribution of groups to the community uptake (Fig. 5). The estimated contribution of small cells measured here could also be biased by active cells passing through GF/F filters (Bombar et al. 2018). This would lead to an underestimation of the community rates and could explain the picoplankton rates being higher than community rates at some stations (Fig. 5). Using the cells outlined from nanoSIMS images, we measured that 54% of the non-pigmented prokaryotes, 31% of the *Prochlorococcus* and 7% of the *Synechococcus* cells had an equivalent spherical diameter lower than the 0.7 µm nominal porosity of GF/F filters (Fig. S2) which is in line with previous reports showing that up to ~50% of the non-pigmented prokaryotes and <10% of the cyanobacteria cells eventually pass through GF/F filters (Lee et al. 1995; Morán et al. 1999; Bombar et al. 2018). The combustion of GF/F filters might decrease the nominal pore size (Nayar and Chou 2003). In the future, the use of silver filters with a pore size of 0.2 µm or the Advantex glass fiber filters with a nominal pore size of 0.3 µm (both compatible with elemental analyzers) could reduce the number of cells passing through the filters (Bombar et al. 2018).

411 Based on the relatively low leucine uptake rates in the open ocean (Zubkov et al. 2008), we added leucine
412 at saturating (or close to saturating) concentrations of 10 nmol L^{-1} in order to ensure significant isotopic
413 signal in our samples. The rates provided thus reflect "potential" rates rather than absolute rates. The
414 leucine community uptake rates measured here (0.1-0.3 nmol leucine L^{-1} h^{-1}) are at the higher end of
415 those reported using trace levels isotopes additions (i.e. additions of leucine < 0.5 nmol L^{-1}) in N.
416 Atlantic with the more sensitive radiotracer assays (~0.01-0.1 nmol leucine L^{-1} h^{-1}) (Zubkov et al. 2003;
417 Mary et al. 2008; Hill et al. 2013). Addition of leucine at saturating concentration (20 nmol L^{-1}) in the
418 N. Atlantic resulted in a doubling of leucine uptake rates as compared to those obtain from trace level
419 additions (0.4 nmol L^{-1}) (Hill et al. 2013). This provides some insight into the extent of the rate
420 overestimation presented in our study.

421 ***Could the low N availability explain the dominance of small plankton groups?***

422 The single cell isotopic approach used here provides an estimate of the substrate specific uptake rate. If
423 the only source of C for the pigmented cells is from C-fixation, C-fixation based division rates should
424 reflect division rates at steady-state. For pigmented groups, C-fixation based division rates measured in
425 our study (0.18-0.64 d^{-1}) are in line with previous measurements made in the N. Pacific using the same
426 approach (0.32-0.50 d^{-1}) (Berthelot et al 2019). In our study, C-fixation based division rates were higher
427 for *Synechococcus* (0.45±0.22 d^{-1} on average) than for the two other pigmented groups (0.28±0.12 d^{-1}
428 on average) investigated. This is consistent with patterns and values reported in the review of Kirchman
429 (2016).

430 While C-specific fixation did not appear to scale with cell size at the intra-group level, clear patterns
431 were observed for N-specific uptake rates (Fig. 4). Such a relationship could be explained by nutrient
432 availability. Under nutrient scarcity, small size plankton have a competitive advantage due to their high
433 surface-area-to-volume ratios (Naselli-Flores et al. 2007). At the time of sampling, N species
434 concentrations were low with the sum of NO_3^-, NH_4^+ and N-urea below <200 nmol N L^{-1}. At such low
435 N concentrations, the uptake is limited by the molecular diffusion of N compounds to their cellular
436 membranes (Karp-Boss et al. 1996; Olofsson et al. 2019). Using a diffusion model (see details in

Materials and Methods section), we calculated that cells with a diameter larger than 5 µm could not maintain N-specific NH_4^+ uptake as high as those measured here for pico-plankton. Similar thresholds were found for NO_3^- uptake (7 µm) and N-urea uptake (12 µm). Below these thresholds, smaller cells still profit from their high surface-area-to-volume ratio which could explain the overall inter- and/or intra-group patterns of increasing N-specific uptake with decreasing cell size up to ~1-2 µm equivalent spherical diameter (Fig. 4). Below this limit, the reduction in size for pigmented organisms is limited by non-scalable cellular components, in particular photosynthetic apparatus (Ward et al. 2017). The peak around 1-2 µm equivalent spherical diameter in N-specific rates observed here for pigmented organisms is lower than a previous report in the Mediterranean lagune (2-3 µm) (Bec et al. 2008). This is consistent with an adaptation of the present communities to extremely oligotrophic conditions where further cell size reduction to cope with nutrients scarcity is hindered by minimal maintenance of cellular basal functions. In the case of non-pigmented prokaryote, the more streamlined genome and metabolic functions of this group as compared to cyanobacteria and to a larger extent to photosynthetic pico-eukaryotes allow them a smaller cell size (Swan et al. 2013) and could explain their relatively high efficiency at using leucine available at extremely low concentrations in the ocean (<1 nM, Zubkov et al 2008). Taken together these observations largely explain the numerical dominance of pico-plankton in the oceanic regions sampled. It also implies that, to compensate for their lack of N acquisition competitiveness, larger photosynthetic plankton cells have to rely on alternative strategies such as increasing their surface-area-to-volume ratios by developing complex nanostructure shapes (Mitchell et al. 2013), relying on predation (Stoecker et al. 2017) or symbioses with N_2 fixing organisms (Foster et al. 2011; Zehr et al. 2017).

The relative importance of organic and inorganic sources of C

We measured some C-fixation for a subset of the cells of the non-pigmented prokaryotes group at all stations (15% on average, Fig. 2). This C-fixation by the non-pigmented prokaryotes group may stem from the transfer of ^{13}C fixed by the photosynthetic organisms during the incubation (Arandia-Gorostidi et al. 2017) or an active fixation performed by chemoautotrophs such as nitrifying bacteria (Middelburg 2011). Despite conservative sorting procedures, it is also possible that pigmented organisms were

missorted in the non-pigmented prokaryotes group. However, at the group scale, C-fixation by non-pigmented prokaryotes were not statistically significant and trivial in comparison to uptake by their photosynthetic counterparts, in line with the expected partitioning between pigmented and non-pigmented organisms with respect to C-fixation.

C-specific leucine potential uptake rates by non-pigmented prokaryotes were on average 4–10 times higher than those of pigmented groups (Fig. 2, Table S3) confirming the competitive advantage of heterotrophs in the acquisition of organic molecules such as leucine. C-specific leucine potential uptake rates in pigmented groups were low but statistically significant at the single cell level for 14-53% of the pigmented cells and at the group level at most sites (see criteria in material and methods section) (Table S3). This use of organic C might explain the survival of photosynthetic pico-eukaryotes in extended darkness such as polar winter (Deventer and Heckman 1996) or the maintenance of active *Prochlorococcus* populations at depth when low light levels limit photosynthetic activity (Coe et al. 2016). The leucine uptake measured in pigmented groups can originate either from a direct osmotrophic uptake of leucine, or indirectly from predation on prey which would have assimilated ^{13}C-leucine during the incubation. Many studies report predation by taxa belonging to the photosynthetic pico-eukaryotes group by phagocytosis (Zubkov et al. 2008; Duhamel et al. 2019), which might explain a fraction of the leucine uptake measured here for this group. On the other hand, direct osmotrophic uptake of dissolved organic compounds by pigmented eukaryotes is common and could also explain the leucine uptake observed in photosynthetic pico-eukaryotes observed in our study (Ruiz-González et al. 2012). More studies are needed to assess the relative importance of phagotrophy and osmotrophy in the mixotrophic strategies of photosynthetic pico-eukaryotes. In the cases of *Prochlorococcus* and *Synechococcus*, leucine uptake is likely through osmotrophy as direct uptake of organic molecules (e.g. glucose, amino acids) has been reported (Muñoz-Marín et al. 2020) while, to the best of our knowledge, predation has not been observed.

The relative importance of organic and inorganic sources of N

In our study, NH_4^+ and urea were the dominant sources of N at the community level (Table 1), in agreement with observations made previously in the gyre and in the Gulf Stream (Lipschultz 2001; Casey et al. 2007). This was also verified at the group level for the pigmented and non-pigmented groups (Fig. 3). The importance of NO_3^- uptake was much more reduced but contrasting patterns were observed between groups. Significant NO_3^- uptake by *Prochlorococcus* confirms previous reports (Casey et al. 2007; Berube et al. 2015; Berthelot et al. 2019). However, NO_3^- only accounted for a small fraction of *Prochlorococcus* N sources (3.7±8.2%, Table 2), in line with previous results using a similar approach in the North Pacific Gyre (4.5±6.5%) (Berthelot et al. 2019). In contrast, NO_3^- represented a larger fraction of N uptake for *Synechococcus* in the North Atlantic (11.5±12.8% on average, this study) than in the North Pacific (2.9±2.1%, Berthelot et al., 2019). This difference may be explained by the greater NO_3^- concentrations in the Atlantic, since in the North Pacific Gyre, surface NO_3^- concentrations remain lower than 10 nmol L^{-1} (Karl et al. 2001). In our study regions, sampled surface waters were depleted in NO_3^- but regular mixing events bring NO_3^- concentrations well above 100 nmol L^{-1} in the mixed layer, even in the GYR (Lipschultz 2001; Treibergs et al. 2014). The transiently more available NO_3^- might result in the adaptation or selection of *Synechococcus* populations that are more efficient at using NO_3^- when available (Casey et al. 2007). This is further confirmed by the generally low $\delta^{15}N$ signature of *Synechococcus* and *Prochlorococcus*, characteristic of a reliance on remineralized N compounds such as NH_4^+ or N-urea (Fawcett et al. 2011). In the presence of NO_3^-, the $\delta^{15}N$ of these groups can increase, confirming the capacity of the organisms to use NO_3^- when available in the North Atlantic Gyre (Fawcett et al. 2011; Treibergs et al. 2014).

Pigmented organisms generally outcompeted non-pigmented prokaryotes for the acquisition of these inorganic N species. N-specific NH_4^+ and NO_3^- uptake rates by non-pigmented prokaryotes were indeed generally lower than in pigmented groups (Fig. 3). The uptake of NH_4^+ and NO_3^- by non-pigmented prokaryotes averaged 7±3% and 2±2% of the community uptake, respectively. These uptake estimates fall at the lower end of previous reported contributions ranging from 5 to 60% for NH_4^+ and 4 to 80% for NO_3^- (Kirchman et al. 1994; Fouilland et al. 2007; Trottet et al. 2011). The differences could be due

to regional variability in dissolved inorganic N concentrations, with our study sites displaying lower concentrations than previous studies which were conducted in more N rich waters. We cannot rule out that discrepancies also result from methodological differences, with previous studies relying mostly on size fractionation or inhibitors. Additional single-cell experiments in N rich waters would help to unravel changes in N-species uptake for different groups as a function of N availability.

Conclusions and implications

In this study, we provided a comprehensive analysis of *in situ* assimilation rates of organic and inorganic C and N sources for different groups of the picoplankton community. A principal component analysis shows the group specific C- and N-trophic strategies (Fig. 6). At the group level pigmented and non-pigmented organisms were clearly partitioned, with the former clustering around C-fixation and NO_3^- and N-urea uptake, and the latter around C- and N-leucine uptake. On the other hand, the principal component analysis shows that NH_4^+ uptake is a poor predictor of the groups' partitions. In contrast to previous findings in the North Pacific (Berthelot et al. 2019), *Synechococcus* appeared to be the group relying the most on NO_3^-. This suggests that the same pico-plankton group might adopt different nutrient uptake strategies between oceanic regions. Intriguingly, *Prochlorococcus* and photosynthetic pico-eukaryotes showed higher C- and N-specific leucine potential uptake than *Synechococcus*. This capacity to diversify their C and N sources, either by osmotrophic uptake or by predation, may allow these microorganisms to maintain their growth under extremely severe nutrient-depleted environments (Zubkov et al. 2003). This behavior could explain the maintenance of the populations and their dominance in some of the most oligotrophic oceanic regimes (Flombaum et al. 2020).

Little is known on variations in nutrition acquisition strategies across environmental gradients, and in particular, across light and nutrients gradients. Taken together, our results provide a snapshot of the picoplankton strategies in the uptake of organic and inorganic sources of C and N. While we observed clear distinctions in C and N uptake strategies between pigmented and non-pigmented groups (Fig. 6), our results also highlight contrasting strategies among the pigmented groups and the importance of cell size in osmotrophic nutrient acquisition (Fig. 6). As a result of global warming, picoplankton is likely

to become more important in ocean biogeochemistry as oligotrophic waters are predicted to expand due to increased water column stratification (Flombaum et al. 2020). A combination of approaches, including those presented here, will be needed to improve our understanding of the key processes (such as nutrient affinity, competition, associations, predation) determining the dynamic of plankton groups and to predict their fate in the context of a changing ocean.

Acknowledgements

We would like to thank the crew of the *R/V Atlantic Explorer* for their help during the cruise. We also thank Smail Mostefaoui for his assistance with the nanoSIMS analyses at the French National Ion MicroProbe Facility hosted by the Muséum National d'Histoire Naturelle (Paris). N. C. and H. B. were supported by the "Laboratoire d'Excellence" LabexMER (ANR-10-LABX-19) and co-funded by a grant from the French government under the program "Investissements d'Avenir". SD was funded by the National Science Foundation (OCE-1434916 and OCE-1458070). The authors declare that there is no conflict of interest.

References

Arandia-Gorostidi, N., P. K. Weber, L. Alonso-Sáez, X. A. G. Morán, and X. Mayali. 2017. Elevated temperature increases carbon and nitrogen fluxes between phytoplankton and heterotrophic bacteria through physical attachment. ISME J. **11**: 641–650. doi:10.1038/ismej.2016.156

Azam, F. 1998. Microbial Control of Oceanic Carbon Flux: The Plot Thickens. Science (80-.). **280**: 694–696. doi:10.1126/science.280.5364.694

Baer, S. E., M. W. Lomas, K. X. Terpis, C. Mouginot, and A. C. Martiny. 2017. Stoichiometry of *Prochlorococcus*, *Synechococcus*, and small eukaryotic populations in the western North Atlantic Ocean. Environ. Microbiol. **19**: 1568–1583. doi:10.1111/1462-2920.13672

Bec, B., Y. Collos, A. Vaquer, D. Mouillot, and P. Souchu. 2008. Growth rate peaks at intermediate cell size in marine photosynthetic picoeukaryotes. Limnol. Oceanogr. **53**: 863–867. doi:10.4319/lo.2008.53.2.0863

566 Berg, G. M., P. M. Glibert, M. W. Lomas, and M. A. Burford. 1997. Organic nitrogen uptake and
567 growth by the chrysophyte *Aureococcus anophagefferens* during a brown tide event. Mar. Biol.
568 **129**: 377–387. doi:10.1007/s002270050178

569 Berthelot, H., S. Duhamel, S. L'Helguen, J.-F. Maguer, S. Wang, I. Cetinić, and N. Cassar. 2019.
570 NanoSIMS single cell analyses reveal the contrasting nitrogen sources for small phytoplankton.
571 ISME J. **13**: 651–662. doi:10.1038/s41396-018-0285-8

572 Berube, P. M., S. J. Biller, A. G. Kent, and others. 2015. Physiology and evolution of nitrate
573 acquisition in *Prochlorococcus*. ISME J. **9**: 1195–1207. doi:10.1038/ismej.2014.211

574 Bombar, D., R. W. Paerl, R. Anderson, and L. Riemann. 2018. Filtration via Conventional Glass Fiber
575 Filters in $^{15}N_2$ Tracer Assays Fails to Capture All Nitrogen-Fixing Prokaryotes. Front. Mar. Sci.
576 **5**. doi:10.3389/fmars.2018.00006

577 Bradley, P. B., M. W. Lomas, and D. A. Bronk. 2010. Inorganic and Organic Nitrogen Use by
578 Phytoplankton Along Chesapeake Bay, Measured Using a Flow Cytometric Sorting Approach.
579 Estuaries and Coasts **33**: 971–984. doi:10.1007/s12237-009-9252-y

580 Bronk, D. A., J. H. See, P. Bradley, and L. Killberg. 2007. DON as a source of bioavailable nitrogen
581 for phytoplankton. Biogeosciences **4**: 283–296. doi:10.5194/bg-4-283-2007

582 Casey, J. R., K. M. Björkman, S. Ferrón, and D. M. Karl. 2019. Size dependence of metabolism within
583 marine picoplankton populations. Limnol. Oceanogr. **64**: 1819–1827. doi:10.1002/lno.11153

584 Casey, J. R., M. W. Lomas, J. Mandecki, and D. E. Walker. 2007. *Prochlorococcus* contributes to new
585 production in the Sargasso Sea deep chlorophyll maximum. Geophys. Res. Lett. **34**: L10604.
586 doi:10.1029/2006GL028725

587 Coe, A., J. Ghizzoni, K. LeGault, S. Biller, S. E. Roggensack, and S. W. Chisholm. 2016. Survival of
588 *Prochlorococcus* in extended darkness. Limnol. Oceanogr. **61**: 1375–1388.
589 doi:10.1002/lno.10302

590 Deventer, B., and C. W. Heckman. 1996. Effects of prolonged darkness on the relative pigment
591 content of cultured diatoms and green algae. Aquat. Sci. **58**: 241–252. doi:10.1007/BF00877511

592 Du, H., N. Jiao, Y. Hu, and Y. Zeng. 2006. Diversity and distribution of pigmented heterotrophic
593 bacteria in marine environments. FEMS Microbiol. Ecol. **57**: 92–105. doi:10.1111/j.1574-
594 6941.2006.00090.x

595 Duhamel, S., E. Kim, B. Sprung, and O. R. Anderson. 2019. Small pigmented eukaryotes play a major
596 role in carbon cycling in the P-depleted western subtropical North Atlantic, which may be
597 supported by mixotrophy. Limnol. Oceanogr. **64**: 2424–2440. doi:10.1002/lno.11193

598 Fawcett, S. E., M. W. Lomas, J. R. Casey, B. B. Ward, and D. M. Sigman. 2011. Assimilation of
599 upwelled nitrate by small eukaryotes in the Sargasso Sea. Nat. Geosci. **4**: 717–722.
600 doi:10.1038/ngeo1265

601 Flombaum, P., W.-L. Wang, F. W. Primeau, and A. C. Martiny. 2020. Global picophytoplankton niche
602 partitioning predicts overall positive response to ocean warming. Nat. Geosci. **13**: 116–120.
603 doi:10.1038/s41561-019-0524-2

604 Foster, R. A., M. M. M. Kuypers, T. Vagner, R. W. Paerl, N. Musat, and J. P. Zehr. 2011. Nitrogen
605 fixation and transfer in open ocean diatom-cyanobacterial symbioses. ISME J. **5**: 1484–93.
606 doi:10.1038/ismej.2011.26

607 Fouilland, E., M. Gosselin, R. B. Rivkin, C. Vasseur, and B. Mostajir. 2007. Nitrogen uptake by
608 heterotrophic bacteria and phytoplankton in Arctic surface waters. J. Plankton Res. **29**: 369–376.
609 doi:10.1093/plankt/fbm022

610 Fukuda, R., H. Ogawa, T. Nagata, and I. Koike. 1998. Direct Determination of Carbon and Nitrogen
611 Contents of Natural Bacterial Assemblages in Marine Environments. Appl. Environ. Microbiol.
612 **64**: 3352–3358. doi:10.1128/AEM.64.9.3352-3358.1998

613 Gradoville, M. R., D. Bombar, B. C. Crump, R. M. Letelier, J. P. Zehr, and A. E. White. 2017.
614 Diversity and activity of nitrogen-fixing communities across ocean basins. Limnol. Oceanogr.

615 **62**: 1895–1909. doi:10.1002/lno.10542

616 Harrison, W. G., L. R. Harris, and B. D. Irwin. 1996. The kinetics of nitrogen utilization in the oceanic
617 mixed layer: Nitrate and ammonium interactions at nanomolar concentrations. Limnol.
618 Oceanogr. **41**: 16–32. doi:10.4319/lo.1996.41.1.0016

619 Hartmann, M., C. Grob, G. A. Tarran, A. P. Martin, P. H. Burkill, D. J. Scanlan, and M. V. Zubkov.
620 2012. Mixotrophic basis of Atlantic oligotrophic ecosystems. Proc. Natl. Acad. Sci. **109**: 5756–
621 5760. doi:10.1073/pnas.1118179109

622 Hernández-Ruiz, M., E. Barber-Lluch, A. Prieto, X. A. Álvarez-Salgado, R. Logares, and E. Teira.
623 2018. Seasonal succession of small planktonic eukaryotes inhabiting surface waters of a coastal
624 upwelling system. Environ. Microbiol. **20**: 2955–2973. doi:10.1111/1462-2920.14313

625 Hill, P. G., P. E. Warwick, and M. V. Zubkov. 2013. Low microbial respiration of leucine at ambient
626 oceanic concentration in the mixed layer of the central Atlantic Ocean. Limnol. Oceanogr. **58**:
627 1597–1604. doi:10.4319/lo.2013.58.5.1597

628 Holmes, R. M., A. Aminot, R. Kérouel, B. a Hooker, and B. J. Peterson. 1999. A simple and precise
629 method for measuring ammonium in marine and freshwater ecosystems. Can. J. Fish. Aquat. Sci.
630 **56**: 1801–1808. doi:10.1139/f99-128

631 Ibarbalz, F. M., N. Henry, M. C. Brandão, and others. 2019. Global Trends in Marine Plankton
632 Diversity across Kingdoms of Life. Cell **179**: 1084-1097.e21. doi:10.1016/j.cell.2019.10.008

633 Jardillier, L., M. V Zubkov, J. Pearman, and D. J. Scanlan. 2010. Significant CO_2 fixation by small
634 prymnesiophytes in the subtropical and tropical northeast Atlantic Ocean. ISME J. **4**: 1180–1192.
635 doi:10.1038/ismej.2010.36

636 Kamjunke, N., B. Köhler, N. Wannicke, and J. Tittel. 2008. Algae as competitors for glucose with
637 heterotrophic bacteria. J. Phycol. **44**: 616–623. doi:10.1111/j.1529-8817.2008.00520.x

638 Karl, D. M., K. M. Björkman, J. E. Dore, L. Fujieki, D. V Hebel, T. Houlihan, R. M. Letelier, and L.

639 M. Tupas. 2001. Ecological nitrogen-to-phosphorus stoichiometry at station ALOHA. Deep. Res.
640 Part II Top. Stud. Oceanogr. **48**: 1529–1566. doi:10.1016/S0967-0645(00)00152-1

641 Karp-Boss, L., E. Boss, and P. A. Jumars. 1996. Nutrient fluxes to planktonic osmotrophs in the
642 presence of fluid motion. Oceanogr. Mar. Biol. an Annu. Rev. **34**: 71–101.

643 Kellogg, C. T. E., and J. W. Deming. 2009. Comparison of free-living, suspended particle, and
644 aggregate-associated bacterial and archaeal communities in the Laptev Sea. Aquat. Microb. Ecol.
645 doi:10.3354/ame01317

646 Kirchman, D. L., H. W. Ducklow, J. J. McCarthy, and C. Garside. 1994. Biomass and nitrogen uptake
647 by heterotrophic bacteria during the spring phytoplankton bloom in the North Atlantic Ocean.
648 Deep. Res. Part I **41**: 879–895. doi:10.1016/0967-0637(94)90081-7

649 Kirchman, D. L., and P. A. Wheeler. 1998. Uptake of ammonium and nitrate by heterotrophic bacteria
650 and phytoplankton in the sub-Arctic Pacific. Deep. Res. Part I Oceanogr. Res. Pap. **45**: 347–365.
651 doi:10.1016/S0967-0637(97)00075-7

652 Klawonn, I., N. Nahar, J. Walve, and others. 2016. Cell-specific nitrogen- and carbon-fixation of
653 cyanobacteria in a temperate marine system (Baltic Sea). Environ. Microbiol. **18**: 4596–4609.
654 doi:10.1111/1462-2920.13557

655 Lee, S., Y. C. Kang, and J. A. Fuhrman. 1995. Imperfect retention of natural bacterioplankton cells by
656 glass fiber filters. Mar. Ecol. Prog. Ser. doi:10.3354/meps119285

657 Li, Y. H., and S. Gregory. 1974. Diffusion of ions in sea water and in deep-sea sediments. Geochim.
658 Cosmochim. Acta **38**: 703–714. doi:10.1016/0016-7037(74)90145-8

659 Lipschultz, F. 2001. A time-series assessment of the nitrogen cycle at BATS. Deep. Res. Part II Top.
660 Stud. Oceanogr. **48**: 1897–1924. doi:10.1016/S0967-0645(00)00168-5

661 Longsworth, L. G. 1963. Diffusion in the water-methanol system and the Walden product. J. Phys.
662 Chem. doi:10.1021/j100797a036

663 Marañón, E. 2015. Cell Size as a Key Determinant of Phytoplankton Metabolism and Community
664 Structure. Ann. Rev. Mar. Sci. **7**: 241–264. doi:10.1146/annurev-marine-010814-015955

665 Martiny, A. C., C. T. A. Pham, F. W. Primeau, J. A. Vrugt, J. K. Moore, S. A. Levin, and M. W.
666 Lomas. 2013. Strong latitudinal patterns in the elemental ratios of marine plankton and organic
667 matter. Nat. Geosci. **6**: 279–283. doi:10.1038/ngeo1757

668 Mary, I., G. A. Tarran, P. E. Warwick, M. J. Terry, D. J. Scanlan, P. H. Burkill, and M. V. Zubkov.
669 2008. Light enhanced amino acid uptake by dominant bacterioplankton groups in surface waters
670 of the Atlantic Ocean. FEMS Microbiol. Ecol. doi:10.1111/j.1574-6941.2007.00414.x

671 Massana, R. 2011. Eukaryotic Picoplankton in Surface Oceans. Annu. Rev. Microbiol. **65**: 91–110.
672 doi:10.1146/annurev-micro-090110-102903

673 Middelburg, J. J. 2011. Chemoautotrophy in the ocean. Geophys. Res. Lett. **38**.
674 doi:10.1029/2011GL049725

675 Mitchell, J. G., L. Seuront, M. J. Doubell, D. Losic, N. H. Voelcker, J. Seymour, and R. Lal. 2013.
676 The Role of Diatom Nanostructures in Biasing Diffusion to Improve Uptake in a Patchy Nutrient
677 Environment. PLoS One. doi:10.1371/journal.pone.0059548

678 Moore, C. M., M. M. Mills, R. Langlois, A. Milne, E. P. Achterberg, J. La Roche, and R. J. Geider.
679 2008. Relative influence of nitrogen and phosphorus availability on phytoplankton physiology
680 and productivity in the oligotrophic sub-tropical North Atlantic Ocean. Limnol. Oceanogr.
681 doi:10.4319/lo.2008.53.1.0291

682 Moore, J. K., R. J. Geider, C. Guieu, and others. 2013. Processes and patterns of nutrient limitation.
683 Nat. Geosci. **6**: 1–10. doi:10.1038/NGEO1765

684 Morán, X. A. G., J. M. Gasol, L. Arin, and M. Estrada. 1999. A comparison between glass fiber and
685 membrane filters for the estimation of phytoplankton POC and DOC production. Mar. Ecol.
686 Prog. Ser. doi:10.3354/meps187031

687 Moutin, T., P. Raimbault, and J.-C. Poggiale. 1999. Primary production in surface waters of the
688 western Mediterranean sea. Calculation of daily production. Comptes Rendus l'Académie des
689 Sci. - Ser. III - Sci. la Vie **322**: 651–659.

690 Mucko, M., S. Bosak, R. Casotti, C. Balestra, and Z. Ljubešić. 2018. Winter picoplankton diversity in
691 an oligotrophic marginal sea. Mar. Genomics **42**: 14–24. doi:10.1016/j.margen.2018.09.002

692 Mulvenna, P. F., and G. Savidge. 1992. A modified manual method for the determination of urea in
693 seawater using diacetylmonoxime reagent. Estuar. Coast. Shelf Sci. **34**: 429–438.
694 doi:10.1016/S0272-7714(05)80115-5

695 Muñoz-Marín, M. C., G. Gómez-Baena, A. López-Lozano, J. A. Moreno-Cabezuelo, J. Díez, and J.
696 M. García-Fernández. 2020. Mixotrophy in marine picocyanobacteria: use of organic compounds
697 by Prochlorococcus and Synechococcus. ISME J. **14**: 1065–1073. doi:10.1038/s41396-020-0603-
698 9

699 Naselli-Flores, L., J. Padisák, and M. Albay. 2007. Shape and size in phytoplankton ecology: do they
700 matter? Hydrobiologia **578**: 157–161. doi:10.1007/s10750-006-2815-z

701 Nayar, S., and L. M. Chou. 2003. Relative efficiencies of different filters in retaining phytoplankton
702 for pigment and productivity studies. Estuar. Coast. Shelf Sci. doi:10.1016/S0272-
703 7714(03)00075-1

704 Olofsson, M., E. K. Robertson, L. Edler, L. Arneborg, M. J. Whitehouse, and H. Ploug. 2019. Nitrate
705 and ammonium fluxes to diatoms and dinoflagellates at a single cell level in mixed field
706 communities in the sea. Sci. Rep. doi:10.1038/s41598-018-38059-4

707 Oremland, R. S., and D. G. Capone. 1988. Use of "Specific" Inhibitors in Biogeochemistry and
708 Microbial Ecology, p. 285–383. *In* Advances in Microbial Ecology.

709 Otero-Ferrer, J., P. Cermeño, A. Bode, and others. 2018. Factors controlling the community structure
710 of picoplankton in contrasting marine environments. Biogeosciences **15**: 6199–6220.
711 doi:10.5194/bg-15-6199-2018

712 Raimbault, P., G. Slawyk, B. Coste, and J. Fry. 1990. Feasibility of using an automated colorimetric
713 procedure for the determination of seawater nitrate in the 0 to 100 n M range: Examples from
714 field and culture. Mar. Biol. **104**: 347–351. doi:10.1007/BF01313277

715 Ruiz-González, C., M. Galí, E. Sintes, G. J. Herndl, J. M. Gasol, and R. Simó. 2012. Sunlight Effects
716 on the Osmotrophic Uptake of DMSP-Sulfur and Leucine by Polar Phytoplankton. PLoS One.
717 doi:10.1371/journal.pone.0045545

718 Sanders, R. W., and R. J. Gast. 2012. Bacterivory by phototrophic picoplankton and nanoplankton in
719 Arctic waters. FEMS Microbiol. Ecol. doi:10.1111/j.1574-6941.2011.01253.x

720 Schapira, M., C. D. McQuaid, and P. W. Froneman. 2012. Metabolism of free-living and particle-
721 associated prokaryotes: Consequences for carbon flux around a Southern Ocean archipelago. J.
722 Mar. Syst. doi:10.1016/j.jmarsys.2011.08.009

723 Sedwick, P. N., P. W. Bernhardt, M. R. Mulholland, R. G. Najjar, L. M. Blumen, B. M. Sohst, C.
724 Sookhdeo, and B. Widner. 2018. Assessing Phytoplankton Nutritional Status and Potential
725 Impact of Wet Deposition in Seasonally Oligotrophic Waters of the Mid-Atlantic Bight.
726 Geophys. Res. Lett. **45**: 3203–3211. doi:10.1002/2017GL075361

727 Seymour, J. R., S. A. Amin, J. B. Raina, and R. Stocker. 2017. Zooming in on the phycosphere: The
728 ecological interface for phytoplankton-bacteria relationships. Nat. Microbiol.
729 doi:10.1038/nmicrobiol.2017.65

730 Stoecker, D. K., P. J. Hansen, D. A. Caron, and A. Mitra. 2017. Mixotrophy in the Marine Plankton.
731 Ann. Rev. Mar. Sci. doi:10.1146/annurev-marine-010816-060617

732 Strickland, J. D. H., and T. R. Parson. 1972. A Practical Handbook of Seawater Analysis, Fisheries
733 Research Board of Canada.

734 Swan, B. K., B. Tupper, A. Sczyrba, and others. 2013. Prevalent genome streamlining and latitudinal
735 divergence of planktonic bacteria in the surface ocean. Proc. Natl. Acad. Sci. U. S. A.
736 doi:10.1073/pnas.1304246110

737 Treibergs, L. a., S. E. Fawcett, M. W. Lomas, and D. M. Sigman. 2014. Nitrogen isotopic response of
738 prokaryotic and eukaryotic phytoplankton to nitrate availability in Sargasso Sea surface waters.
739 Limnol. Oceanogr. **59**: 972–985. doi:10.4319/lo.2014.59.3.0972

740 Trottet, A., E. Fouilland, C. Leboulanger, E. Lanouguère, and M. Bouvy. 2011. Use of inhibitors for
741 coastal bacteria and phytoplankton: Application to nitrogen uptake measurement. Estuar. Coast.
742 Shelf Sci. **93**: 151–159. doi:10.1016/j.ecss.2011.04.007

743 Ward, B. A., E. Marañón, B. Sauterey, J. Rault, and D. Claessen. 2017. The size dependence of
744 phytoplankton growth rates: A trade-off between nutrient uptake and metabolism. Am. Nat.
745 doi:10.1086/689992

746 Wu, J., W. Sunda, E. A. Boyle, and D. M. Karl. 2000. Phosphate depletion in the Western North
747 Atlantic Ocean. Science (80-.). doi:10.1126/science.289.5480.759

748 Zehr, J. P., I. N. Shilova, H. M. Farnelid, M. del C. Muñoz-Marín, and K. A. Turk-Kubo. 2017.
749 Unusual marine unicellular symbiosis with the nitrogen-fixing cyanobacterium UCYN-A. Nat.
750 Microbiol. **2**: 16214. doi:10.1038/nmicrobiol.2016.214

751 Zubkov, M. V. 2014. Faster growth of the major prokaryotic versus eukaryotic CO_2 fixers in the
752 oligotrophic ocean. Nat. Commun. **5**. doi:10.1038/ncomms4776

753 Zubkov, M. V., B. M. Fuchs, G. A. Tarran, P. H. Burkill, and R. Amann. 2003. High rate of uptake of
754 organic nitrogen compounds by *Prochlorococcus* cyanobacteria as a key to their dominance in
755 oligotrophic oceanic waters. Appl. Environ. Microbiol. **69**: 1299–1304.
756 doi:10.1128/AEM.69.2.1299-1304.2003

757 Zubkov, M. V., G. A. Tarran, I. Mary, and B. M. Fuchs. 2008. Differential microbial uptake of
758 dissolved amino acids and amino sugars in surface waters of the Atlantic Ocean. J. Plankton Res.
759 **30**: 211–220. doi:10.1093/plankt/fbm091

760

Tables

Table 1. Biogeochemistry of the six stations investigated. All the samples were collected in triplicates (average ± standard deviation), unless otherwise stated. ND: not detected.

	Temperature (°C)	Particulate C (µmol C L^{-1})	Concentrations (nmol N L^{-1} or nmol P L^{-1})				Abundances (10^3 cell mL^{-1})				Community uptake rates (nmol C L^{-1} h^{-1} or nmol N L^{-1} h^{-1})					
			$Nitrate^-$	Ammonium	Urea	Phosphate	Non-pigmented prokaryotes	*Prochlorococcus*	*Synechococcus*	Photosynthetic pico-eukaryotes	C-fixation	Nitrate uptake	Ammonium uptake	Urea uptake	C-leucine potential uptake	N-leucine potential uptake
Station								**North Atlantic Gyre**								
A	27.8	2.0±0.2	<10	15±1	92±54	15±3*	243±10	11.0±0.9	9.7±1.7	0.5±0.1	18.7±2.8	0.4±0.1	1.0±0.4	1.0±0.5	0.2±0.0	0.1±0.0
B	27.8	1.9±0.2	<10	11±2	173±7	18±4*	252±19	12.2±0.7	8.2±0.9	0.4±0.0	20.2±2.0	0.4±0.1	1.7±0.3	1.8±0.2	0.2±0.1	0.1±0.1
								Gulf Stream								
C	26	4.0±0.2	<10	11±5	163±47	40±2*	584±15	207.6±18.0	26.8±3.0	1.6±0.4	66.7±3.3	0.9±0.0	3.0±0.2	6.3±0.7	0.4±0.1	0.1±0.1
D	23.3	3.5±0.2	<10	18±7	91±14	45±4*	381±18	38.2±5.8	57.7±2.8	1.7±0.2	64.6±4.1	1.4±0.6	4.8±1.5	7.0±1.8	0.5±0.1	0.2±0.1
								Continental Shelf								
E	16.8	11.7±1.5	<10	17±0	144±33	152±4*	609±65	ND	53.7±5.4	12.2±2.1	162.0±7.8	3.8±1.1	6.1±0.8	9.8±3.3	0.8±0.3	0.3±0.2
F	18.8	8.3±1.8	<10	28±7	106±7	110±2*	297±12	ND	26.6±1.9	4.7±1.0	121.6±19.7	3.7±0.4	23.6±5.0	11.0±2.9	0.7±0.1	0.3±0.1

* Duplicate samples.

765 Table 2. Relative importance of the different N sources investigated (average ± standard deviation
766 between stations, in %) for the N acquisition budget of each group.

	Ammonium	**Nitrate**	**N-urea**	**N-leucine**
Non-pigmented prokaryotes	50.2±66.2	2.1±1.6	37.6±28.6	10.1±3.6
Prochlorococcus	34.3±21.5	3.7±8.2	61.1±69.9	0.9±0.4
Synechococcus	29.3±32.4	11.5±12.8	59.0±54.2	0.3±0.6
Photosynthetic pico-eukaryotes	54.7±57.6	9.2±10.1	35.1±31.7	1.0±0.6

767

768

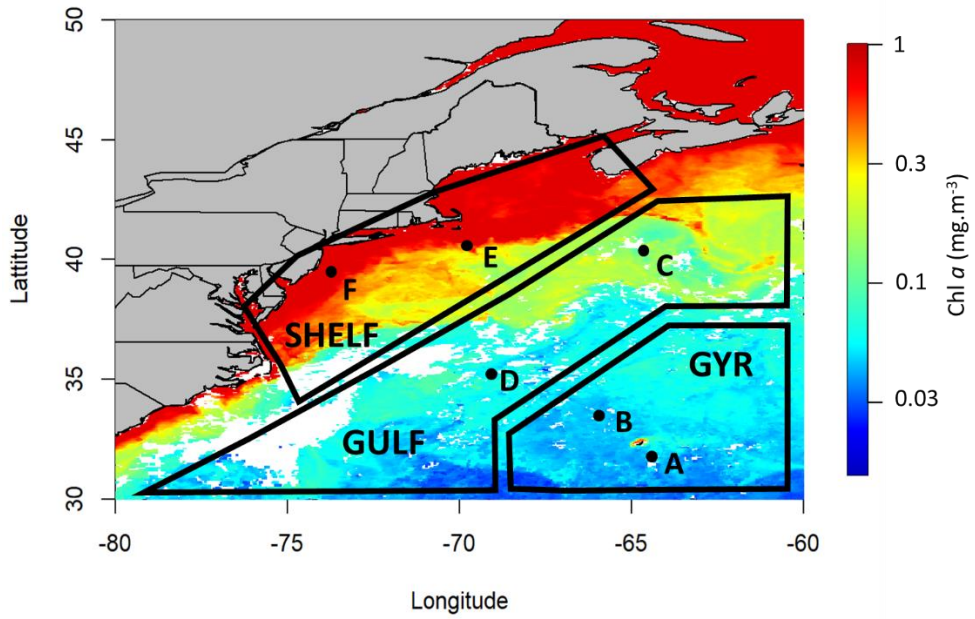

769

770 Figure 1. Location of the stations and the oceanic regions sampled in the northwestern Atlantic Ocean
771 (SHELF: continental shelf, GULF: Gulf Stream, GYR: North Atlantic Gyre) superimposed on surface
772 chlorophyll a (Chl a) concentration (in $mg.m^{-3}$) from AQUA/MODIS (composite image of August
773 2017).

774

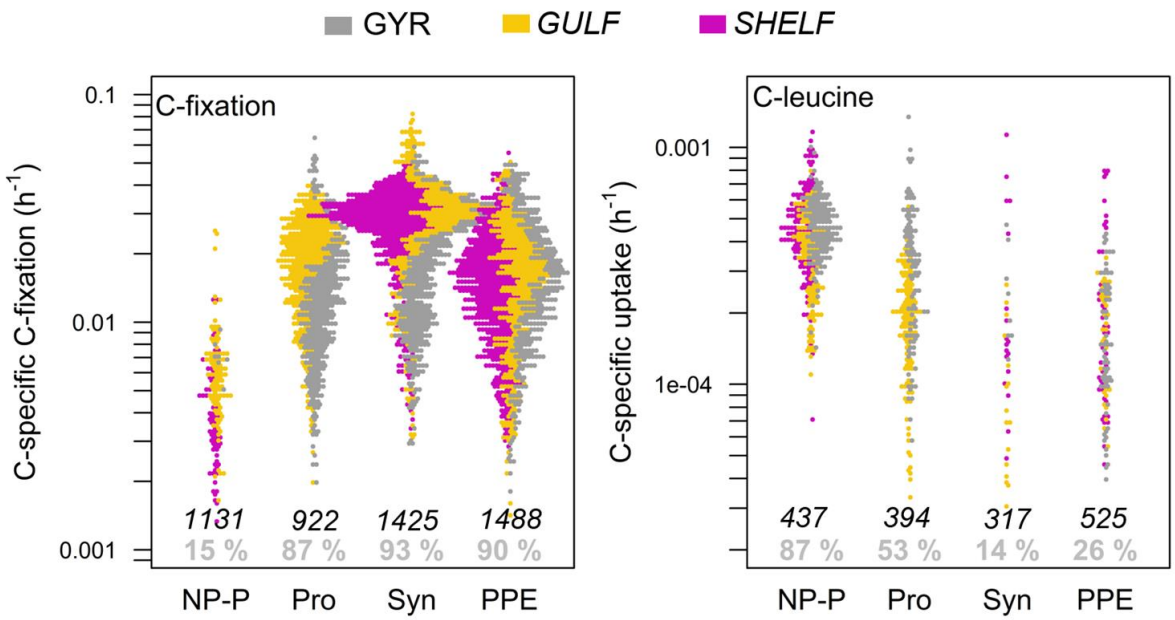

775

776 Figure 2. Single cell C-specific C-fixation rates and C-specific leucine potential uptake rates (h^{-1}) for
777 each group investigated (NP-P: non-pigmented prokaryotes, Pro: *Prochlorococcus*, Syn:
778 *Synechococcus*, PPE: photosynthetic pico-eukaryotes). Each point represents an analyzed cell. Only the
779 cells with detected activity with respect to the process under study are shown. Italic black numbers
780 denote the number of cells analyzed for each group. Grey numbers denote the proportion (in %) of cells
781 for which activity was detected. Colors denote the sampling regions (North Atlantic Gyre (GYR), Gulf
782 Stream (GULF) and continental shelf (SHELF) in grey, yellow and purple, respectively). Note the order
783 of magnitude difference between the two-logarithm y-scales.

784

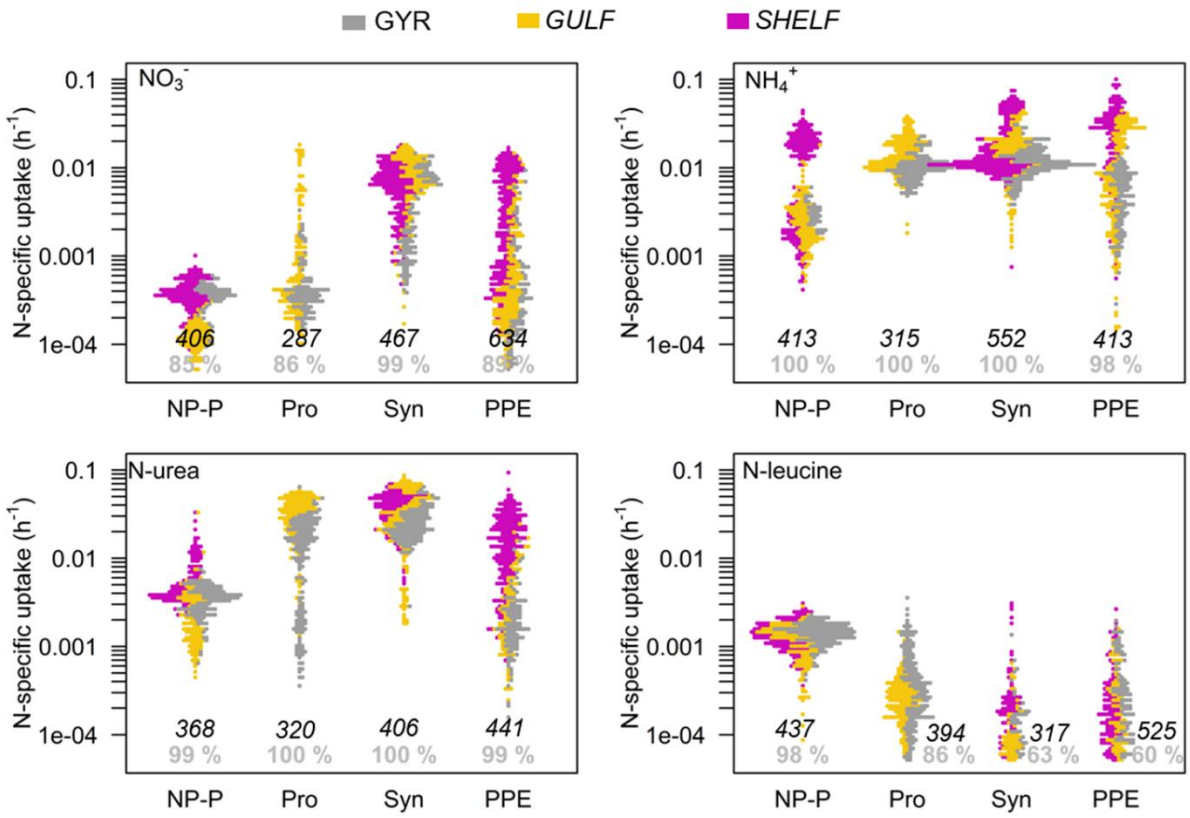

785

786 Figure 3. Single cell N-specific nitrate (NO_3^-), ammonium (NH_4^+), urea and leucine specific uptake rates
787 (h^{-1}) for each group (NP-P: non-pigmented prokaryotes, Pro: *Prochlorococcus*, Syn: *Synechococcus*,
788 PPE: photosynthetic pico-eukaryotes). Each point represents an analyzed cell. Only the cells with
789 detected activity with respect to the process under study are shown. Italic black numbers denote the
790 number of cells analyzed for each group. Grey numbers denote the proportion (in %) of cells for which
791 activity was detected. Colors denote the sampling regions (North Atlantic Gyre (GYR), Gulf Stream
792 (GULF) and continental shelf (SHELF) in grey, yellow and purple, respectively).

793

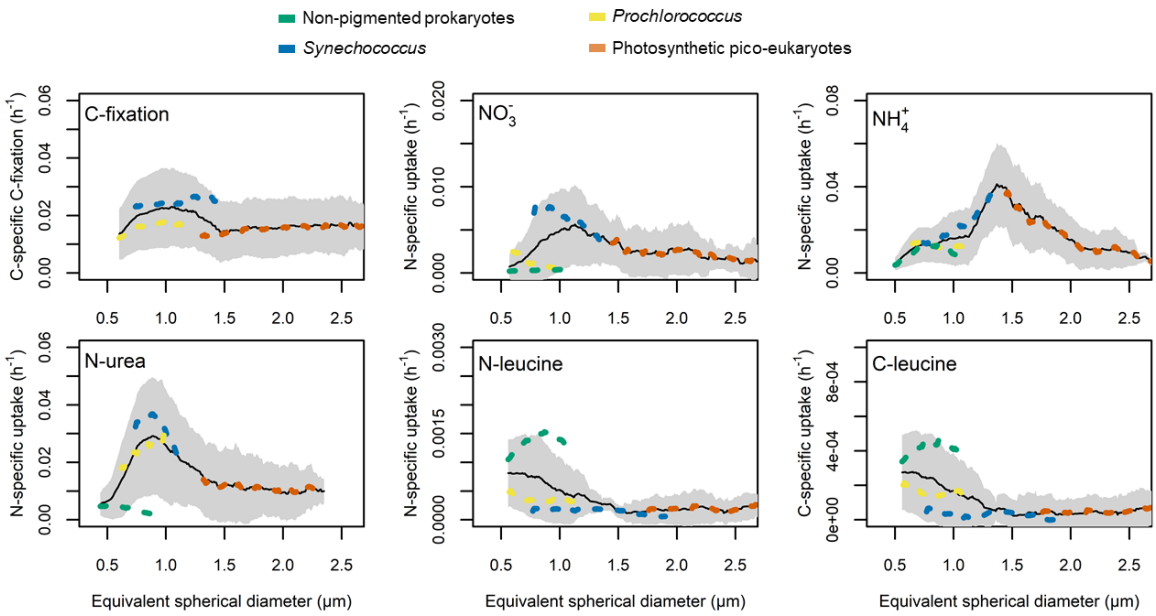

794

795 Figure 4. Single cell C- and N-specific C-fixation, nitrate (NO_3^-), ammonium (NH_4^+), urea and leucine
796 uptake rates (h^{-1}) as a function of cell size. The black lines and the shaded area denote the average and
797 standard deviation of rates for all the groups analyzed (except non-pigmented prokaryotes in the case of
798 C-fixation). Colored dashed lines denote group specific uptake rates (non-pigmented prokaryotes,
799 *Prochlorococcus*, *Synechococcus* and photosynthetic pico-eukaryotes in green, yellow, blue and red,
800 respectively).

801

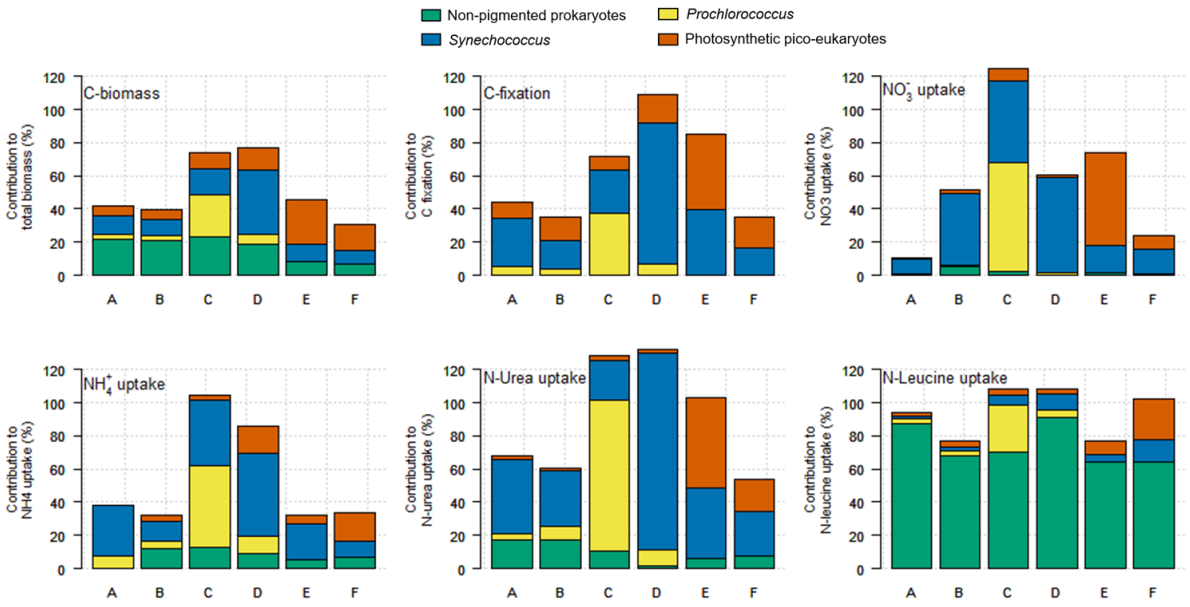

Figure 5. Contribution of picoplankton groups to the community C-biomass, C-fixation, nitrate (NO_3^-), ammonium (NH_4^+), N-urea and N-leucine uptake rates at each station investigated. Colors denote the analyzed groups (non-pigmented prokaryotes, *Prochlorococcus*, *Synechococcus* and photosynthetic pico-eukaryotes in green, yellow, blue and red, respectively).

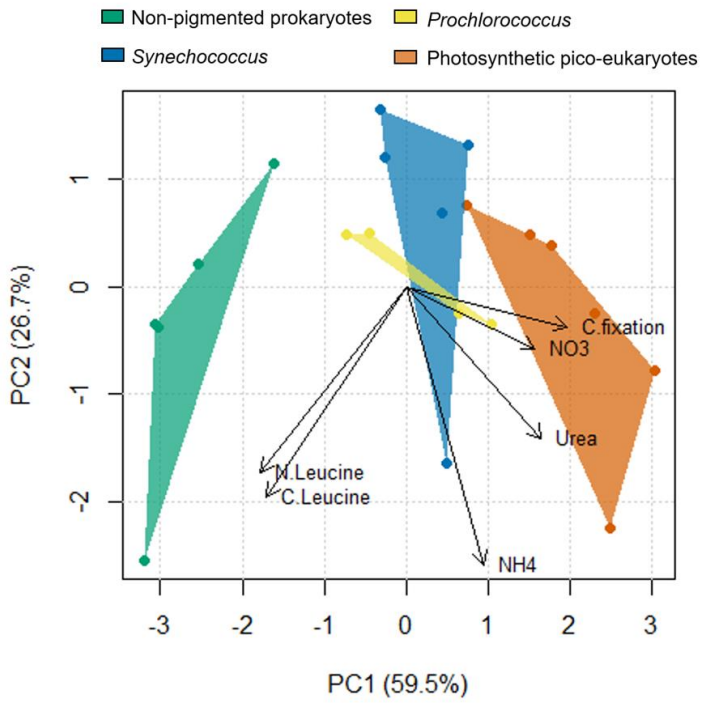

808

809 Figure 6. Principal Component Analysis of the C- and N-specific uptake rates highlighting the
810 differences in C and N strategies of the different groups investigated (data were normalized and
811 centered). Each point represents a group at a given sampling station.

812